

Analysis of a sandwich-type generator with self-heating thermoelectric elements



Mikyung Kim^a, Hyein Yang^a, Daehyun Wee^{a,b,*}

^a Department of Environmental Science and Engineering, Ewha Womans University, Seoul 120-750, Republic of Korea

^b Ewha Global Top 5 Research Program, Ewha Womans University, Seoul 120-750, Republic of Korea

ARTICLE INFO

Article history:

Received 13 August 2013

Accepted 16 February 2014

Available online 17 March 2014

Keywords:

Thermoelectric generators

Radioactive isotopes

Heat transfer

Efficiency

Power density

ABSTRACT

A novel and unique design of thermoelectric generators, in which a heat source is combined with thermoelectric elements, is proposed. By placing heat-generating radioactive isotopes inside the thermoelectric elements, the heat transfer limitation between the generator and the heat source can be eliminated, ensuring simplicity. The inner electrode is sandwiched between identical thermoelectric elements, which naturally allows the inner core to act as the hot side. Analysis shows that conversion efficiency and power density increase as the heat density inside the thermoelectric elements increases and as the thermoelectric performance of the material improves. The theoretical maximum efficiency is shown to be 50%. However, realistic performance under practical constraint is much worse. In realistic cases, the efficiency would be about 3% at best. The power density of the proposed design exhibits a much more reasonable value as high as 3000 W/m². Although the efficiency is low, the simplicity of the proposed design combined with its reasonable power density may result in some, albeit limited, potential applications. Further investigation must be performed in order to realize such potential.

© 2014 Elsevier Ltd. All rights reserved.

1. Introduction

Thermoelectric generators, which utilize thermoelectric materials to convert heat to electricity, provide an alternative option to conventional heat engines in the field of power generation, most notably in compact waste heat recovery systems or in generic power supplies at remote, isolated locations. Typically, the maximum efficiency of thermoelectric energy conversion is presented in terms of the temperature of each heat reservoir and the thermoelectric figure of merit $ZT = S^2T/(\rho k)$, where S is the Seebeck coefficient, ρ is the electric resistivity, k is the thermal conductivity, and T is the temperature, leading to the following traditional expression for the maximum thermoelectric conversion efficiency (η_0) [1]:

$$\eta_0 = \frac{T_h - T_c}{T_h} \frac{\sqrt{ZT + 1} - 1}{\sqrt{ZT + 1} + T_c/T_h}, \quad (1)$$

where ZT is typically evaluated at the mean temperature (T_m) of the hot-side temperature T_h and the cold-side temperature T_c . From the equation, it is clear that the increase of ZT leads to the increase of

* Corresponding author at: Department of Environmental Science and Engineering, Ewha Womans University, Seoul 120-750, Republic of Korea.

E-mail address: dhwee@ewha.ac.kr (D. Wee).

the energy conversion efficiency, and significant efforts have been exerted on creating materials with high ZT values. Nanowires [2], thin films [3], and materials with grain boundaries [4] have also been investigated, showing various degrees of success in improving ZT .

However, conventional thermoelectric generators do not perform as well as promised. Many factors are contributing to the performance gap between the theoretical estimate of thermoelectric materials and the actual performance of conventional thermoelectric generators. One of the most significant contributors is the limited heat transfer between the hot- and/or cold-side thermal reservoirs and the generator itself [5]. Large temperature difference typically occurs between the heat source (or sink) and the generator due to a poor heat transfer coefficient. The actual temperature difference across thermoelectric elements made of thermoelectric materials becomes small as a result. With a small actual temperature difference, the performance of thermoelectric materials, which is relatively poor already, suffers even more in real-world applications.

In this article, we study the feasibility of a self-heating thermoelectric generator, in which thermoelectric materials create their own heat. Since the thermoelectric elements heat themselves, there is no need for engineering a good thermal interface between the hot-side thermal reservoir and the generator, which eliminates the difficulty of achieving good heat transfer, at least on one side.

Self-heating thermoelectric materials are not being utilized yet, but there does exist certain prospect for such development. One potential way to develop such materials is to incorporate radioactive isotopes in traditional thermoelectric materials. For example, a known thermoelectric oxide (SrTiO_3) [6,7] can be altered into a self-heating thermoelectric oxide by replacing regular atoms (Sr) with radioactive isotopes (^{90}Sr). Another method is to fill radioactive isotopes into a skutterudite, which is one of the most promising thermoelectric materials [8]. Radioactive isotopes were previously used as a heat source in the context of thermoelectric generation in space missions [9,10] and in isolated monitoring sites [11]. In particular, the use of ^{90}Sr in the form of SrTiO_3 as a heat source was already reported [12], but combining radioactive isotopes with thermoelectric elements is a possibility that has been hardly explored before.

The paper is organized as follows. In Section 2, first, we describe the proposed design of a thermoelectric generator using self-heating thermoelectric materials. Then, we continue to discuss our method of analysis for evaluating the performance of the generator. In Section 3, the method described in Section 2 is applied while changing the design parameters within realistic ranges in order to evaluate the performance indices of the proposed design. In Section 4, conclusions are drawn by summarizing and discussing the results.

2. Analysis of the proposed design

Our proposed design is presented in Fig. 1. Unlike conventional thermoelectric modules, there is no external heat source other than the self-heating thermoelectric elements inside the generator. Hence, there is no distinction between the hot side and the cold side specified by external thermal reservoirs. Only with appropriate thermal boundary conditions imposed, can a proper temperature difference across a thermoelectric element be developed. The use of a sandwich-like shape, where the inner electrode is located between two identical thermoelectric elements, is used to achieve such boundary conditions in a straightforward fashion. The inner boundary becomes naturally adiabatic, which renders the inner core as the hot side.

For simplicity, we only consider one single unipolar element in our analysis. Since the entire generator is constructed by alternating concatenation of two different types of unipolar elements, the performance of the entire generator can be analyzed by summing the power output of all elements. The governing equation describing the temperature distribution (T) in one single unipolar element is given as follows:

$$\frac{d}{dx} \left(k \frac{dT}{dx} \right) + \rho j^2 + \dot{q} = 0. \quad (2)$$

x is the variable for the outward longitudinal coordinate. k and ρ are the thermal conductivity and the electrical resistivity of the thermoelectric element, respectively. j is the current density, and \dot{q} is the amount of heat generated per unit volume, which is uniform and constant between $x = 0$ and L . Because the purpose of the analysis is a preliminary evaluation of feasibility, only minimal functional features are included in Eq. (2). For instance, the Thomson effect is excluded, although it may affect actual performance [13]. Another effect neglected here is that of interfacial Ohmic heating, which is an important mechanism causing losses in traditional thermoelectric modules, where the leg length of each thermoelectric element is relatively small, like several millimeters. In the present design, however, the leg length must be much larger, since each leg must act as its own heat source as well. As shown in Section 3, the leg length of each thermoelectric element may reach more than 5 cm. Using the value of resistivity in Table 1, the value of the electrical resistance of one leg per unit area is estimated to be $15 \times 10^{-3} \Omega \text{ cm}^2$. It was reported that the interfacial resistance of a typical thermoelectric module is on the order of $10^{-6} \Omega \text{ cm}^2$ [14]. Thus, it is clear that the interfacial Ohmic heating may be neglected without too much loss of generality.

The corresponding boundary conditions are given by:

$$jS - k \frac{dT}{dx} = 0 \quad \text{at } x = 0, \quad (3)$$

and

$$T = T_c \quad \text{at } x = L. \quad (4)$$

Here, S is the Seebeck coefficient of the thermoelectric element, L is the coordinate of the outer boundary, and T_c is the temperature of the cold-side end. The first term on the LHS of Eq. (3) represents the Peltier heat. From Eqs. (2)–(4), dimensionless equations are constructed by defining $\theta = T/T^*$ and $\xi = x/L$. T^* is a characteristic temperature, which is given here as $T^* = \dot{q}L^2/k$. The set of corresponding dimensionless equations are:

$$\frac{d^2\theta}{d\xi^2} + v + 1 = 0, \quad (5)$$

$$\mu\theta - \frac{d\theta}{d\xi} = 0 \quad \text{at } \xi = 0, \quad (6)$$

and

$$\theta = \theta_c \quad \text{at } \xi = 1, \quad (7)$$

where $\theta_c = T_c/T^*$, $\mu = jSL/k$, and $v = \rho j^2/\dot{q}$. The solution to Eqs. (5)–(7) is given as follows:

$$\theta(\xi) = \frac{(1 + \mu\xi)(1 + v + 2\theta_c) - (1 + \mu)(1 + v)\xi^2}{2(1 + \mu)}. \quad (8)$$

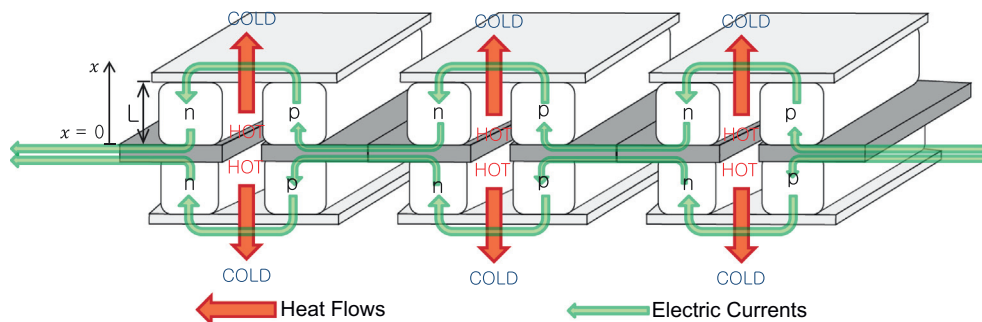


Fig. 1. Schematic illustration of the proposed design of a sandwich-type generator with self-heating thermoelectric elements.

Table 1
Material properties considered.

S ($\mu\text{V/K}$)	ρ ($\Omega\text{ m}$)	k ($\text{W m}^{-1}\text{ K}^{-1}$)	\dot{q} (W/cm^3)
–200	3×10^{-5}	3.5	≤ 0.92

Once the solution is obtained, the temperature distribution can be recovered by converting the result into a dimensional form. Note that, once the material properties (k , \dot{q} , S , and ρ) and the geometry of the generator (L) are specified, μ and v , which have dependency on the operating condition (j), are not independent of each other, since

$$\frac{\mu^2}{v} = \frac{S^2 T^*}{\rho k} = ZT^*. \quad (9)$$

In order to compute the power output per axial unit length, one must specify the condition of the external load. The external load is modeled as a simple electrical resistance per unit area of the generator (R_L), which can be adjusted to ensure the best performance. We define a dimensionless load parameter m as follows:

$$m = \frac{R_L}{R} = \frac{R_L}{\rho L}, \quad (10)$$

where $R = \rho L$ is the electrical resistance of the generator per unit area. The electromotive force induced by the generator is given as follows:

$$\Phi = S(T(0) - T_c), \quad (11)$$

while j is given as follows:

$$j = \frac{\Phi}{R + R_L} = \frac{S(T(0) - T_c)}{R(1 + m)}, \quad (12)$$

from which we get

$$\mu = \frac{ZT^*}{1 + m} (\theta(0) - \theta_c). \quad (13)$$

Therefore, the power output per unit area is given by:

$$\dot{W} = j^2 R_L = \frac{m S^2 (T(0) - T_c)^2}{R(1 + m)^2}. \quad (14)$$

The heat generated by the imbedded heat source in the thermoelectric element per unit area can be evaluated as follows:

$$\dot{Q}_H = \dot{q}L, \quad (15)$$

and the conversion efficiency can be simply given as:

$$\eta = \frac{\dot{W}}{\dot{Q}_H} = \frac{m ZT^*}{(1 + m)^2} (\theta(0) - \theta_c)^2 = \frac{m \mu^2}{ZT^*} = m v. \quad (16)$$

Solving Eqs. (8) and (13) for μ , we get:

$$\mu = \frac{\zeta}{1 + 2m} \left[\sqrt{1 + \frac{ZT^*(1 + 2m)}{\zeta^2}} - 1 \right], \quad (17)$$

where $\zeta = 1 + m + ZT^* \theta_c = 1 + m + ZT_c$. In principle, substitution of Eq. (17) into Eq. (16) leads to an expression of η as a function of m , which can be maximized to yield the maximum conversion efficiency for given geometry and material (k , \dot{q} , S , ρ , and L specified). The resulting expression is, however, too complicated to provide any meaningful interpretation. Instead, we study two limiting cases where ZT^* is either very small ($ZT^* \ll 1$) or very large ($ZT^* \gg 1$).

When $ZT^* \ll 1$, Eq. (17) can be expanded as a series in ZT^* up to the lowest order as follows:

$$\mu \approx \frac{\zeta}{1 + 2m} \left[1 + \frac{ZT^*(1 + 2m)}{2\zeta^2} - 1 \right] = \frac{ZT^*}{2\zeta}, \quad (18)$$

from which η can be approximately obtained as:

$$\eta = \frac{m \mu^2}{ZT^*} \approx \frac{m ZT^*}{4\zeta^2} = \frac{m ZT^*}{4(1 + m + ZT_c)^2}. \quad (19)$$

Eq. (19) attains its maximum at $m = 1 + ZT_c$. The approximate maximum conversion efficiency is given as follows:

$$\eta_0 \approx \frac{ZT^*}{16(1 + ZT_c)}. \quad (20)$$

As expected, Eq. (20) shows that the conversion efficiency increases as the thermoelectric performance and heat source strength increase.

On the other hand, when $ZT^* \gg 1$,

$$\sqrt{1 + \frac{ZT^*(1 + 2m)}{\zeta^2}} - 1 \approx \frac{\sqrt{ZT^*(1 + 2m)}}{\zeta}, \quad (21)$$

and

$$\mu \approx \frac{\zeta}{1 + 2m} \frac{\sqrt{ZT^*(1 + 2m)}}{\zeta} = \sqrt{\frac{ZT^*}{1 + 2m}}. \quad (22)$$

Therefore,

$$\eta = \frac{m \mu^2}{ZT^*} \approx \frac{m}{ZT^*} \frac{ZT^*}{1 + 2m} = \frac{m}{1 + 2m} \leq \frac{1}{2}, \quad (23)$$

which gives the upper limit of the conversion efficiency as $\eta_0 \leq 1/2 = 50\%$. It should be noted that this number is not something that can be boasted of, although it looks high at first glance. In order to obtain this value, the highest temperature in the system must be unlimited, and the thermoelectric performance must be infinitely high. For traditional thermoelectric generators, Eq. (1) would lead to the maximum efficiency of 100% in such a case (T_h/T_c and $ZT \rightarrow \infty$). Eq. (23) rather shows that the present design inherently has a handicap compared to the regular design. The reason for such loss of efficiency can be attributed to the uniform distribution of the heat source. Thermoelectric elements, whose temperature ranges between the highest temperature and the lowest temperature in the system, generates heat in the present design. Thus, the temperature of its heat source cannot be characterized by the highest temperature in the system, and hence the thermodynamic efficiency suffers.¹ On top of that, this number (50%) overestimates the potential, and realistic performance is much worse, as presented in Section 3.

3. Examples

In this section, the performance of the proposed thermoelectric generator is analyzed with varying design parameters. We consider SrTiO_3 as the material for our thermoelectric element, whose properties are summarized in Table 1. The values of S , ρ , and k roughly correspond to the values reported in [7]. The maximum value of \dot{q} is based on the average power density of the $^{90}\text{SrTiO}_3$ pellets with 7% excess TiO_2 used for the SNAP-7A generator [12]. Note that the value of \dot{q} can be tuned down by lowering the content of ^{90}Sr in the material.

The performance of the generator is evaluated as we vary L , m , \dot{q} , and T_c . With the necessary parameters specified, one can first calculate μ using Eq. (17), obtain $\theta(0)$ using Eq. (8), and finally evaluate \dot{W} and η using Eqs. (14) and (16).

While typical elements in conventional thermoelectric modules are only several millimeters long, a length scale of several

¹ Theoretically, it is possible to overcome the handicap of low efficiency by concentrating the heat source near the hot end, which may be a topic for a future investigation.

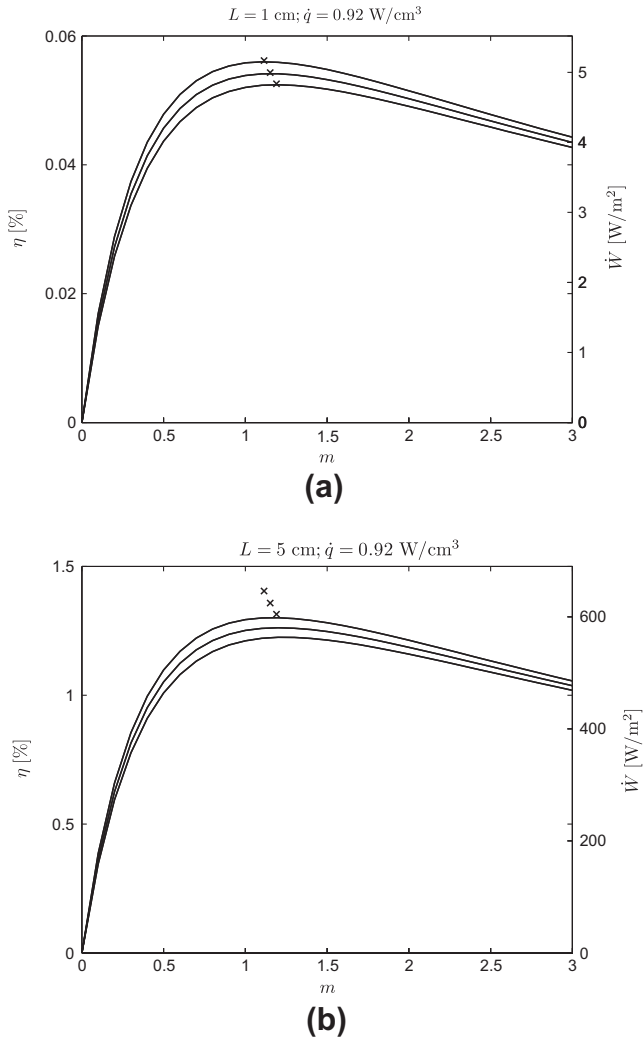


Fig. 2. Typical performance graphs showing efficiency and power density. $\dot{q} = 0.92$ W/cm³. (a) $L = 1$ cm; (b) $L = 5$ cm. In each figure, three curves and three crosses represent the actual performance of the generator and the approximate value, represented by Eq. (20), for each of three values of T_c , which are 300 K (highest performance), 400 K, and 500 K (lowest performance), respectively.

centimeters is more reasonable in our case, where the thermoelectric element also acts as a heat source. In order to generate a significant amount of heat, a heat source must possess a large enough volume. For example, the diameters of the $^{90}\text{SrTiO}_3$ pellets of the SNAP-7A generator were reported to be 3.4–3.8 cm [12]. Cases where $L \leq 10$ cm are considered in this study. T_c is varied between 300 K (room temperature) and 500 K (elevated temperature).²

The performance graphs of typical cases, where $\dot{q} = 0.92$ W/cm³, are provided in Fig. 2. For a given geometry (L), material (S , ρ , k , and \dot{q}), and boundary condition (T_c), the performance graph exhibits one optimal operating condition specified by a particular value of m .

² Although the present design eliminates the thermal interface at the hot side, it still needs to maintain a good thermal interface at the cold side. The condition $T_c = 500$ K is used to address the effect of the thermal resistance at the cold side. As shown later in this section, a typical power output is about 2000 W/m², and, considering the efficiency in the order of 1%, a typical thermal load that must be removed at the heat sink is at most about 0.2 MW/m². This value is much smaller than the critical heat flux in the boiling heat transfer of water at 1 atm (more than 1 MW/m²), which occurs at the excess temperature of 30 °C or equivalently at the surface temperature of 130 °C [15]. 500 K is significantly higher than 130 °C, and hence the effect of a finite heat transfer coefficient through the heat sink is partially addressed.

The operating condition for maximum power output and that for maximum efficiency are identical, since \dot{Q}_H is independent of m , unlike conventional thermoelectric generators where the amount of the heat transfer from the hot-side thermal reservoir depends on the operating condition, i.e., the load resistance. The maximum efficiency of the generator is very low (much less than 1%) especially when ZT^* is small, as shown in Fig. 2(a). Increase in ZT^* by increasing L improves the efficiency, as expected from Eq. (20), but Fig. 2(b) shows that the actual value still remains relatively low ($\approx 1\%$) even with $L = 5$ cm.

The power density is, on the other hand, much better. With $L = 5$ cm, the maximum power density may reach a level beyond 400 W/m², which is the power density of photovoltaic power generation that can be achieved by today's best experimental designs (multi-junction concentrators with efficiency of about 40%) during the peak insolation hours [16]. It should also be noted that the approximate value of the maximum efficiency computed by Eq. (20) is close to the actual value, which suggests that Eq. (20) can be used to roughly estimate the performance of the proposed design, though the difference between the approximate value and the actual value increases as ZT^* increases.

More insight on the way how the generator works can be brought in by looking at a typical temperature profile inside the thermoelectric element, as shown in Fig. 3. There are a few things to remark. First, the temperature profile is parabolic, mainly due to the effect of the heat source embedded in the thermoelectric element. It is a very different profile from the nearly linear shape typically observed in traditional thermoelectric generators [13]. Second, the maximum temperature (T_{max}) occurs not at $x = 0$ but at a point strictly inside ($x = 0.3$ cm in this case), though the difference between T_{max} and $T(0)$ is hardly recognizable (only about 1 K). This is due to the competition between the heat conduction and the Peltier heat at $x = 0$. As one can see from Eq. (3), the incoming Peltier heat must be compensated by the outgoing heat conduction in order to maintain the adiabatic boundary condition. Since the electromotive force given in Eq. (11) is dependent only on the temperature values at the edges, the parabolic shape and the occurrence of T_{max} at a point inside may have a somewhat detrimental effect to the performance of the generator. A way of alleviating such a negative impact can be a topic that should be pursued in a future study.

In order to investigate the maximum efficiency and power density achievable, the performance indices have been computed while the design parameters (L , \dot{q} , T_c) are changed. For each set of design parameters, m is optimized to achieve the maximum

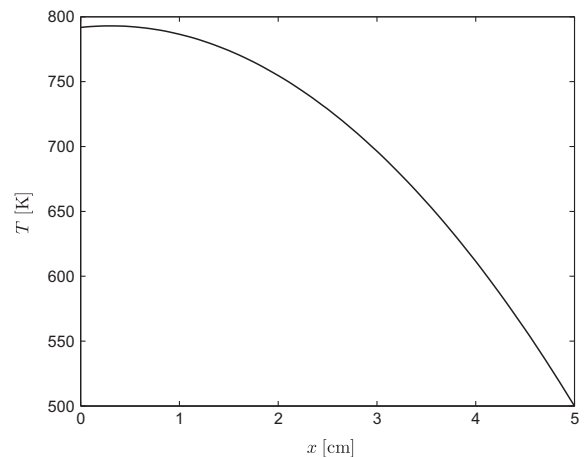


Fig. 3. A typical temperature profile inside the thermoelectric element. $\dot{q} = 0.92$ W/cm³, $L = 5$ cm, $T_c = 500$ K, and $m = 1 + ZT_c$.

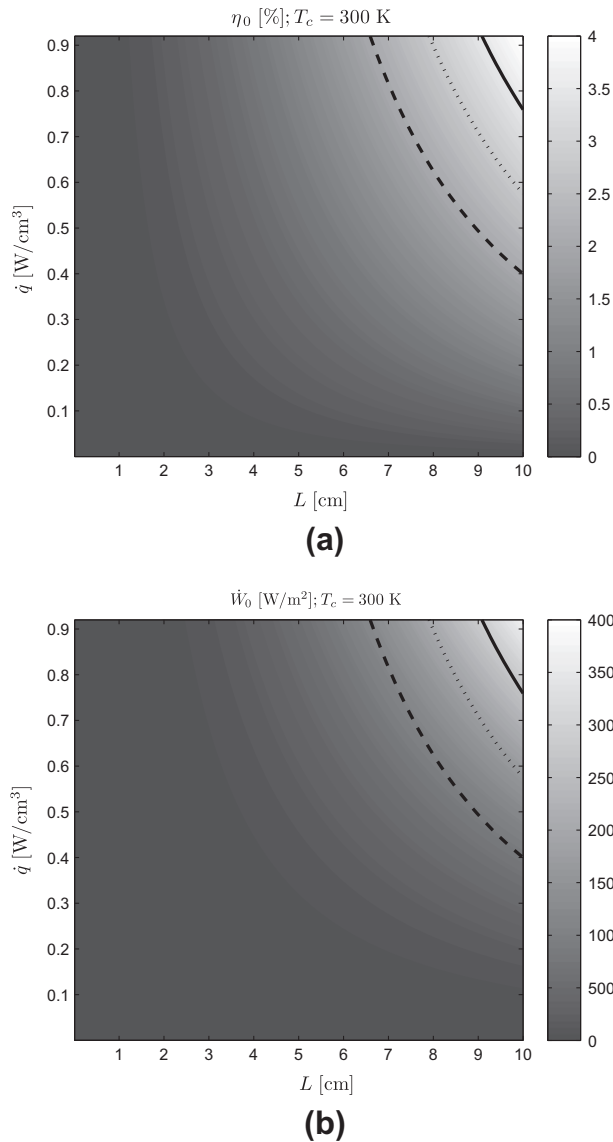


Fig. 4. Contour plots of performance variation in cases where $\dot{q} \leq 0.92$ W/cm³, $L \leq 10$ cm, and $T_c = 300$ K, while m is optimized for the maximum performance. (a) Maximum efficiency and (b) maximum power density. Curves represent the contour lines of $T(0)$ (dashed: 800 K; dotted: 1000 K; solid: 1200 K).

performance. The result for $T_c = 300$ K and that for $T_c = 500$ K are presented in Figs. 4 and 5, respectively. Obviously, the performance indices improve as \dot{q} and L increase, for ZT^* is enhanced in the course. However, unchecked increases of \dot{q} and of L are impossible for several practical reasons. First, as mentioned earlier in this section, \dot{q} can only be tuned down from its maximum value, since the amount of Sr atoms that can be replaced with ⁹⁰Sr atoms is limited. Another rather more significant constraint comes from the consideration of $T(0)$. The increases in \dot{q} and L naturally result in an increase in the temperature of the inner core, which can be detrimental to structural and material integrity of the system. Especially, excessive temperature of the inner electrode may critically affect the stability of the system. Although noble metals, like platinum, rhodium, palladium or iridium, can, in principle, be used to produce high-temperature-stable electrodes, there are both technical and economic challenges in the application of these noble metals [17]. Thus, the maximum attainable value of $T(0)$ should be considered as a limiting constraint here. For this reason, the

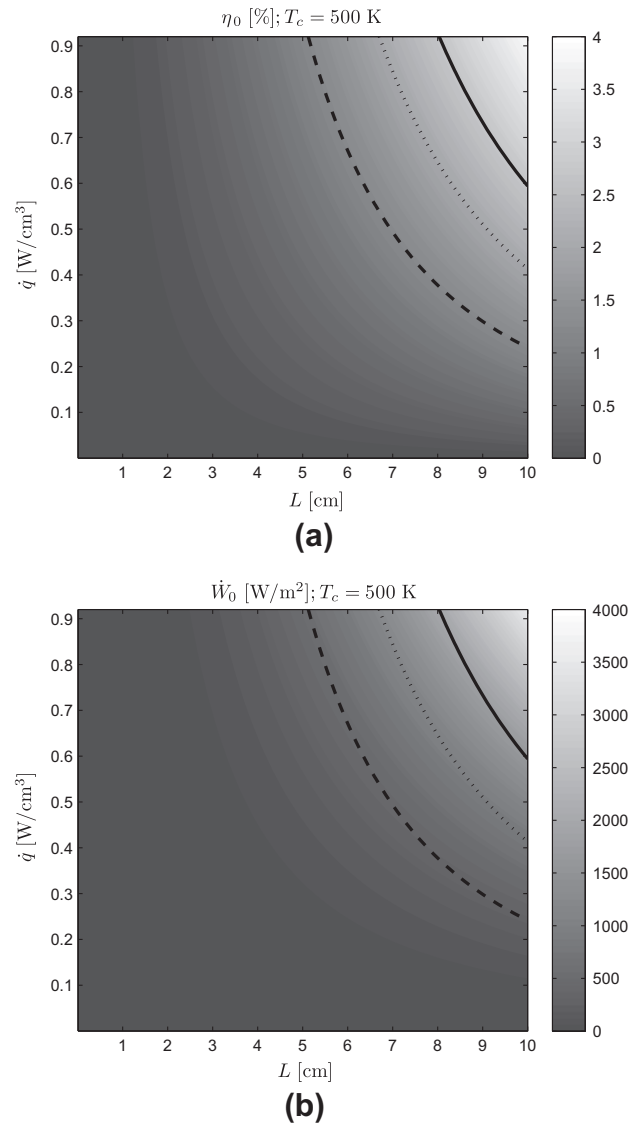


Fig. 5. Contour plots of performance variation. The same convention as in Fig. 4 is employed except for T_c , which is set as $T_c = 500$ K.

contour lines of three values of $T(0)$ (800 K, 1000 K, and 1200 K) are also given in Figs. 4 and 5. Table 2 summarizes the results from Figs. 4 and 5. The results show that the maximum efficiency is more or less limited to the level of 2% or 3%, while the maximum power density may reach around 3000 W/m².

As the last example, we consider a situation close to the condition of an actual radioisotope thermoelectric generator. The comparison is made against the general-purpose heat source radioisotope thermoelectric generator (GPHS-RTG), which was used as the Galileo and Ulysses power sources [9,10]. The GPHS-RTGs were built to deliver approximately 300 W of electrical power with a nominal fuel loading yielding about 4400 W of thermal energy [9,10], yielding an efficiency of 6.82%. Since the thermoelectric uncouples in the GPHS-RTG operated at a nominal 1273 K/573 K hot junction/cold junction in a vacuum environment [9], we set $T_c = 573$ K and $T(0) \leq 1273$ K. The expected performance of our sandwich-type thermoelectric generator in such a condition is reported in Table 3.

The maximum efficiency of the proposed design in the GPHS-RTG-like condition is 2.76%, which is lower than that of the GPHS-RTGs. This result is not surprising. As already mentioned

Table 2Maximum efficiency and power density attainable with $T(0)$ limited. For all cases, $L \leq 10$ cm, and $\dot{q} \leq 0.92$ W/cm³.

T_c (K)	$T(0) \leq 800$ K		$T(0) \leq 1000$ K		$T(0) \leq 1200$ K	
	η_{\max} (%)	\dot{W}_{\max} (W/m ²)	η_{\max} (%)	\dot{W}_{\max} (W/m ²)	η_{\max} (%)	\dot{W}_{\max} (W/m ²)
300	2.04	1199	2.77	1956	3.47	2849
500	1.23	559	1.99	1185	2.72	1989

Table 3Maximum efficiency and power density in the GPHS-RTG-like condition. $\dot{q} \leq 0.92$ W/cm³.

T_c (K)	$T(0)$ (K)	L (cm)	η_{\max} (%)	\dot{W}_{\max} (W/m ²)
573	≤ 1273	8	2.76	2016

earlier in Section 2, it is expected that our sandwich-type thermoelectric generator has a lower thermodynamic efficiency than that of traditional ones. However, since the concept of embedding heat source in thermoelectric elements is new and underdeveloped, there is a room for further design optimization, which may yield future improvement in performance. Additionally, we note that the highest temperature in the entire generator in our case is more or less limited to 1273 K, while the highest temperature occurring in the GPHS-RTG, which would be the temperature at the center of the heat source, must be much higher. Accordingly, thermal and structural issues may become less severe in our design, which can be seen as an advantage over the traditional system.

4. Summary and discussion

In this paper, a new design of thermoelectric generators in which a heat source is combined into thermoelectric elements has been proposed. By placing the heat source inside the thermoelectric elements, the limitation due to heat transfer is only located on the side toward the heat sink, simplifying the overall heat management. The use of radioactive isotopes in conventional thermoelectric materials is proposed as a method of creating such elements. The inner electrode is sandwiched between identical thermoelectric elements, which naturally causes the inner core to act as the hot side.

Our analysis in Section 2 has shown that the performance indices, that is, conversion efficiency and power density, increase as the heat density of the material is increased and the thermoelectric performance is improved. The theoretical maximum efficiency is shown to be 50%. Unfortunately, realistic performance is much worse. As shown in Section 3, the efficiency in realistic cases would be about 3% at best. On the other hand, the power density of the proposed design exhibits a much more reasonable value around 3000 W/m².

Although its efficiency is low, the simplicity of the proposed design combined with its reasonable power density may find some, albeit limited, potential applications, like power generation for control units in isolated storage sites of radioactive nuclear wastes. In order to realize such potential, however, more serious study beyond this preliminary one must be performed. Several technical issues involving the proposed design, which have not been addressed in this preliminary study, may emerge. For instance, potential radiation damages to thermoelectric and other functional materials may place severe limitation on the heat density of the heat source that can be embedded in thermoelectric materials. Radiation-induced segregation and/or void formation [18] may eventually lead to poor thermoelectric performance. Resolution of such issues needs further future investigation.

Acknowledgements

The last author personally dedicates the paper to his family, including his wife, Jiheyon Kim, and his daughter, Seoyeon Wee, for their affection given to him during the course of the study.

Appendix A. A Remark in Eq. (23)

At a glance, Eq. (23) seems to lead to a contradictory conclusion that the maximum efficiency is achieved when $m \rightarrow \infty$, where the power output must become zero. This is, however, only an apparent contradiction. What we have done during the analysis leading to Eq. (23) is asymptotically taking the hypothetical limit of infinitely good thermoelectric performance, in order to identify the absolute maximum efficiency that can be achieved by the present design. For any finite ZT^* , the maximum efficiency is achieved not at $m = \infty$ but at a finite value of m . This can be shown by expanding Eq. (21) up to the next order, as follows:

$$\sqrt{1 + \frac{ZT^*(1+2m)}{\zeta^2}} - 1 \approx \frac{\sqrt{ZT^*(1+2m)}}{\zeta} \left[1 - \frac{\zeta}{\sqrt{ZT^*(1+2m)}} \right], \quad (24)$$

which gives the following expression for μ :

$$\mu \approx \sqrt{\frac{ZT^*}{1+2m}} \left[1 - \frac{\zeta}{\sqrt{ZT^*(1+2m)}} \right]. \quad (25)$$

Therefore,

$$\eta \approx \frac{m}{1+2m} \left[1 - \frac{\zeta}{\sqrt{ZT^*(1+2m)}} \right]^2, \quad (26)$$

where $\zeta = 1 + m + ZT_c$. Under the condition of $T_c/T^* \rightarrow 0$ and $ZT^* \rightarrow \infty$, the value of m that maximizes Eq. (26) is given as follows:

$$m \approx \left(\frac{ZT^*}{2} \right)^{\frac{1}{3}}. \quad (27)$$

Therefore, with a large but finite ZT^* given, the value of m that yields the maximum efficiency also remains, albeit large, finite.

The seemingly contradictory phenomenon is physically caused by the competition between the heat conduction and the Peltier heat at $x = 0$, as shown in Eq. (3). As we increase j , the associated Peltier heat becomes large, making $T(0)$ lower than T_{\max} . Since the power output and the efficiency are all affected by $T(0)$, as in Eqs. (14) and (16), the increase of the Peltier heat at $x = 0$ adversely affects the performance indices. At a very high ZT^* , where such an adverse effect can become significant, m must become relatively large to avoid a negative consequence.

References

- [1] Goldsmid HJ. Conversion efficiency and figure-of-merit. In: Rowe DM, editor. CRC handbook of thermoelectrics. CRC Press; 1995. p. 19–25.
- [2] Wu YY, Fan R, Yang PD. Block-by-block growth of single-crystalline Si/SiGe superlattice nanowires. Nano Lett 2002;2:83–6.
- [3] Venkatasubramanian R, Siivola E, Colpitts T, O'Quinn B. Thin-film thermoelectric devices with high room-temperature figures of merit. Nature 2001;413:597–602.

- [4] Poudel B, Hao Q, Ma Y, Lan YC, Minnich A, Yu B, et al. High-thermoelectric performance of nanostructured bismuth antimony telluride bulk alloys. *Science* 2008;320:634–8.
- [5] Mayer PM, Ram RJ. Optimization of heat sink-limited thermoelectric generators. *Nanoscale Microscale Thermophys Eng* 2006;10:143–55.
- [6] Okuda T, Nakanishi K, Miyasaka S, Tokura Y. Large thermoelectric response of metallic perovskites: $\text{Sr}_{1-x}\text{La}_x\text{TiO}_3$ ($0 \leq x \leq 0.1$). *Phys Rev B* 2001;63:113104.
- [7] Ohta S, Nomura T, Ohta H, Hirano M, Hosono H, Koumoto K. Large thermoelectric performance of heavily Nb-doped SrTiO_3 epitaxial film at high temperature. *Appl Phys Lett* 2005;87(9):092108.
- [8] Nolas GS, Morelli DT, Tritt TM. Skutterudites: a phonon-glass–electron-crystal approach to advanced thermoelectric energy conversion applications. *Ann Rev Mater Sci* 1999;29:89–116.
- [9] Bennett GL, Hemler RJ, Schock A. Development and use of the Galileo and Ulysses power sources. *Space Technol* 1995;15:157–74.
- [10] Furlong RR, Wahlquist EJ. U.S. space missions using radioisotope power systems. *Nucl News* 1999;42:26–34.
- [11] U.S. Congress, Office of Technology Assessment. Power sources for remote arctic applications. Tech. rep. OTA-BP-ETI 129, Washington (DC): U.S. Congress; June 1994.
- [12] Shar R, Lafferty Jr, RH, Baker S. Strontium-90 heat sources. Tech. rep. ORNL-IIC-36, Oak Ridge (TN): Oak Ridge National Laboratory; May 1971.
- [13] Wee D. Analysis of thermoelectric energy conversion efficiency with linear and nonlinear temperature dependence in material properties. *Energy Convers Manage* 2011;52(12):3383–90.
- [14] Gupta RP, McCarty R, Sharp J. Practical contact resistance measurement method for bulk Bi_2Te_3 -based thermoelectric devices. *J Electron Mater* (<http://dx.doi.org/10.1007/s11664-013-2806-6>).
- [15] Incropera FP, DeWitt DP, Bergman TL, Lavine AS. Fundamentals of heat and mass transfer. 6th ed. New York (USA): Wiley; 2006 [chap. 10].
- [16] Smil V. Energy transitions: history, requirements, prospects. Westport (Connecticut, USA): Praeger; 2010. p. 117.
- [17] Richter D, Fritze H. High-temperature stable electrodes for langasite based surface acoustic wave devices. In: Proceedings SENSOR 2011, vol. D1; 2011. p. 532–37.
- [18] Was GS. Fundamentals of radiation material science: metals and alloys. Berlin (Germany): Springer; 2007 [chap. 6 and 8].